Journal of Materials Chemistry B

Accepted Manuscript

This article can be cited before page numbers have been issued, to do this please use: S. NAG, L. DUARTE, E. BERTRAND, V. Celton, M. Castro, V. Choudhary, P. Guegan and J. FELLER, *J. Mater. Chem. B*, 2014, DOI: 10.1039/C4TB01041H.

ROYAL SOCIETY OF CHEMISTRY

www.rsc.org/materialsB

View Article Online
DOI: 10.1039/C4TB01041H

Graphical Abstract

A novel approach to control the multiscale architecture of quantum chemo-resistive transducers is introduced by the supramolecular assembly of graphene and cyclodextrin (CD) derived hybrids. Tailorable selectivity to cancer biomarkers could be achieved due to the insertion of CD with varying functionality between graphene foils.

Keyword: anticipated diagnosis; functional cyclodextrins; graphene; cancer biomarkers; electronic nose

Sananda Nag,[a,b] Lisday Duarte,[c] Emilie Bertrand,[c] Véronique Celton,[c] Mickaël Castro,[a] Veena Choudhary,[b] Philippe Guegan, *[d,e] Jean-François Feller*[a]

Ultrasensitive QRS made by supramolecular assembly of functionalized cyclodextrins and graphene for the detection of lung cancer VOC biomarkers

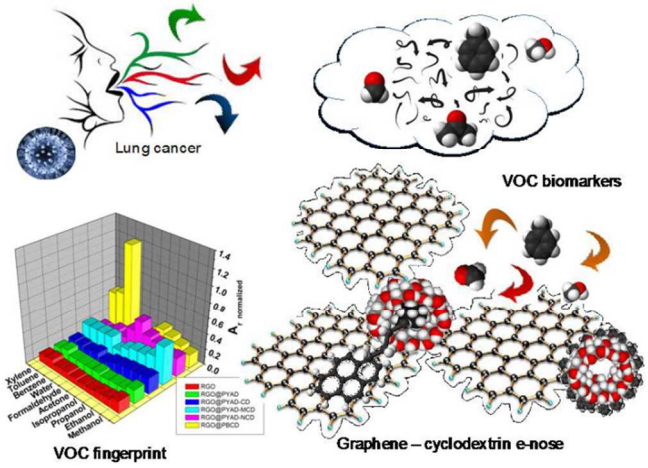

Dynamic Article Links ▶
View Article Online
DOI: 10.1039/C4TB01041H

Cite this: DOI: 10.1039/c0xx00000x

www.rsc.org/xxxxxx

ARTICLE TYPE

Ultrasensitive QRS made by supramolecular assembly of functionalized cyclodextrins and graphene for the detection of lung cancer VOC biomarkers

Sananda Nag,[a,b] Lisday Duarte,[c] Emilie Bertrand,[c] Véronique Celton,[c] Mickaël Castro,[a] Veena Choudhary,[b] Philippe Guegan*[d,e] and Jean-François Feller*[a]

Received (in XXX, XXX) Xth XXXXXXXXX 20XX, Accepted Xth XXXXXXXXX 20XX
DOI: 10.1039/b000000x

A novel electronic nose system comprising functionalized β-cyclodextrin wrapped reduced graphene oxide (RGO) sensors with distinct ability of discrimination of a set of volatile organic compounds, has been developed. Non-covalent modification of chemically functionalized cyclodextrin with RGO is carried out by using pyrene adamantan as a linker wherever necessary, in order to construct a supra molecular assembly. The chemical functionality on cyclodextrin is varied utilising the principle of selective chemical modification of cyclodextrin. In the present study, the combined benefits of host-guest inclusion complex formation ability and tunable chemical functionality of cyclodextrin, as well as high surface area and electrical conductivity of graphene are utilized for the development of a set of highly selective quantum resistive chemical vapour sensors (QRS), which can be assembled in an electronic nose.

1. Introduction

Enhancing the quality of life by decreasing the impact of severe diseases is still a global challenge. According to the World Health Organization (WHO), cancers which are killing each year 7.6 million people can be considered as a global priority.[1] The WHO has also projected that without immediate action, the global number of deaths from cancer will increase by nearly 80 % by 2030, with most occurring in low- and middle-income countries. Cancers could be more efficiently treated in case of an anticipated diagnosis, and from this point of view metabolomics can bring very promising solutions. This new and active field of research is studying the volatile organic compounds (VOC) produced by a biological system to investigate the metabolite differences between natural and perturbed systems (cells, organs and tissues). Thus, metabolomics allows profiling diseases such as cancer from a VOC fingerprint found in breath, urine, faeces, saliva, nasal mucus or gaseous excretions of the skin[2] or combination of them.[3] Among these, exhaled breath is an excellent source containing several hundreds of VOC (including water) but at the ppm or ppb level, which makes their identification difficult. However, analyzing VOC profiles with pattern recognition algorithms allows to efficiently discriminate between cancerous and healthy subjects.[4–13] Nevertheless, the commonly used techniques for breath VOC analysis such as GC-MS,[14] infrared spectroscopy,[15] ion flow tube mass spectrometry,[16] optical spectroscopy,[17] suffer from several shortcomings such as high cost, low-portability, low sensitivity or high consumption. On the contrary, arrays of nonspecific sensors, i.e., electronic noses (e-nose), have demonstrated their effectiveness in the detection of VOC.[18] E-noses present in particular the advantage of being non-invasive, cost effective, quick and portable. Additionally they are allowing real time monitoring[19] and provide almost directly a pattern of exhaled biomarkers in the form of a VOC breath print.[20] Moreover, a wide choice of vapour sensors can be assembled in the array, depending on the nature of the transducer: metal oxides (MO),[20-21] intrinsically conductive polymers (ICP),[22-23] and functionalized carbon nanomaterials or nanocomposites.[25–29] However, e-noses have also some drawbacks, such as processing and performance reproducibility, drift in baseline and response of sensors requiring sometimes recalibration. MO sensors often have a low sensitivity, a lack of selectivity, a high operating temperature (several hundred degrees) imposed by their too high sensitivity to water,[30] whereas ICP sensors are too sensitive to humidity, irradiation and oxido-reduction.[31] Most of these problems can be overcome when using quantum resistive sensors (QRS), which are versatile nanomaterials obtained by the structuring of conductive nanofillers like carbon nanotubes (CNT) into an insulating matrix like a polymer of suitable functionality, provided that a control of both the conductive architecture [30-31] and the nanoswitching at junctions of percolated nanofillers[32-33] is ensured. In addition, the selectivity of QRS can be easily adjusted by changing the chemical nature of the thin organic layer separating the conductive junctions.[34-35] The first problem can be fixed by using a process such as spray layer by layer (sLbL), which allows a step by step building of the transducers from the nano to the macro

View Article Online
DOI: 10.1039/C4TB01041H

scale,[36–38] whereas the second can find a solution through the tailoring of junction's gap.[39,40] This last parameter will determine both the selectivity (depending on the nature of intermolecular interactions between the organic layer and the biomarker) and the sensitivity (depending on the initial value and amplitude of the gap) of QRS.

Several strategies have already been experimented to control the nanoswitching of QRS involving exclusion volumes,[26,33,41] functionalization of carbon nanofillers such as CNT[41,42] or graphene[38] with a polymer,[43–45] an oligomer[42] or nonpolymer organic/inorganic molecules[46–49], which could effectively modify the selectivity and sensitivity of chemo-resistive vapour sensors. However, non-covalent functionalization of nanofillers, which can also be obtained through secondary interactions such as π-π stacking, charge-charge interaction and hydrogen bonding, is probably the most attractive approach to preserve the graphitic chemical structure, and hence, provide a positive synergy of properties.[50]

However, none of these strategies really allow controlling simultaneously the architecture of the conducting network and the physico-chemical properties of the junction's gap, optimizing at the same time sensitivity, stability and selectivity of the QRS. The objective of the present work is to demonstrate that these parameters can be optimized, through the development of hybrid transducers, fabricated by supramolecular assembly of graphene and cyclodextrin. These two singular nanofillers, which combine steric and chemical effects, will allow reaching a positive synergy thanks to their complementary properties that will be shortly described in the following.

Since its discovery in 2004 by GEIM et al.[51] graphene has continuously demonstrated exceptional intrinsic properties such as: high electrical and thermal conductivity (respectively 7200 $S.m^{-1}$ and 5000 $W.m^{-1}.K^{-1}$)[52,53], high aspect ratio (surface area of 2630 $m^2.g^{-1}$ for a thickness of 1nm),[54] mechanical strength (130 GPa),[55] optical transmittance, high carrier mobility and charge carrier concentration at room temperature (250,000 $cm^2.V^{-1}.s^{-1}$).[51] In particular the combination of high electrical conductivity and large specific surface has made graphene an attractive nanomaterial for chemical sensing applications,[56] since the adsorption of individual gas molecules onto a graphene based transducer brings about significant changes in electrical resistance.[57] Moreover, the high carrier mobility of graphene,[58,59] allows room temperature detection and high signal to noise ratio of the resistive sensors.[60] Moreover, It has been found that the non-covalent modification of reduced graphene oxide (RGO) with different functional molecules was helping to prevent the restacking of individual graphene sheets, and was improving both sensitivity and selectivity of the graphene based QRS to different VOC.[61]

β-cyclodextrin (CD) is a cyclic oligosaccharide having a toroidal shape. β-CD is composed of 7 D-glucopyranosidic units containing a hydrophobic internal cavity and a hydrophilic outer side with primary and secondary hydroxyl groups on narrower and wider side respectively. The presence of hydroxyl groups on the outer surface not only makes CD water soluble but also makes it eligible for regio-selective chemical modification,[62] while the hydrophobic internal cavity provides an ability to form host/guest inclusion complexes with various organic, inorganic, biological molecules and polymers showing high molecular selectivity.[63] The main driving forces for the host/guest inclusion complex formation are hydrophobic interactions, van der WAALS interactions or hydrogen bonding. Various fields of applications of chemically modified CD include drug delivery,[64] catalysis,[65] artificial channels[66] and sensing.[67]

A synergistic effect between RGO (due to high conductivity and high surface area) and native CD (thanks to host-guest recognition and enrichment) has been anticipated in 2010 by GUO et al.,[68] who found that RGO-CD hybrids simply prepared by dispersing CD in a graphene oxide (GO) solution followed by the reduction of GO, led to interesting electrochemical response towards biomolecules and drugs, unlike unmodified graphene or carbon nanotubes. LEGER et al., demonstrated that triazole group of functionalized CD may interact with MWCNT by π-π interaction, thus acting as a good dispersing agent that could potentially introduce new recognition sites on the surface of MWCNT.[69] Additionally, KONG et al. have successfully grafted monofunctional-CD derivatives onto SWCNT (Single wall carbon nanotube) by in situ diazonium reaction, to synthesize novel SWCNT-CD with excellent sensitivity and selectivity towards organic pollutants, thanks to molecular recognition.[70] MWCNT (multi walled carbon nanotubes) was also functionalized with monofunctional CD, dangling on the MWCNT and thus providing an easy access to the cavity of the CD.[71] YANG et al. also reported adsorption of a protein, bovine serum albumin, on these functionalized MWCNT through non-covalent interactions with CD derivatives functionalized aligned carbon nanotubes for the electrochemical sensing of DNA via host–guest recognition.[72] Their study recalls that the diazonium reaction does not allow the formation of a single layer of cyclodextrin on the carbon nanotubes, which may limit the performances of the detection. Finally, GUO et al. modified native CD with a pyrene residue to allow the adsorption of the pyrene labeled cyclodextrin on SWCNT to prepare light-switchable SWCNT.[73] However, the reported modifications of graphene or CNT for sensing applications are not versatile, and can only be dedicated to one kind of detection. Furthermore, no chemo-resistive sensing application has been investigated with cyclodextrin functionalized conductive nanocomposites so far.

The originality of the present work is to take benefit from the multiscale architecture of quantum chemo-resistive transducers resulting from the supramolecular assembly of graphene and CD-derivate hybrids, to get a high sensitivity of the nanoswitching at junctions due to the insertion of CD between graphene foils and to obtain a tailorable selectivity to cancer biomarkers due to CD functionalization and geometry. This strategy includes the effectiveness of spray layer by layer to maintain the nanomaterial's properties across the different scales (from nano to micro) and the versatility of non-covalent bonding of functionalized-CD onto graphene via a pyrene spacer (by π-π stacking), which preserve at the same time the integrity of conducting foils and manages to some extent junctions' gap. Moreover, RGO-CD is expected to combine two types of molecular recognitions, non-specific via van der WAALS interactions and specific reversible chemical reactions with CD functions, coming for instance from a free amino group that can react with acetone.

Dynamic Article Links View Article Online
DOI: 10.1039/C4TB01041H

Cite this: DOI: 10.1039/c0xx00000x

www.rsc.org/xxxxxx

ARTICLE TYPE

2. Results and Discussion

2.1. Selection of VOC Lung Cancer Biomarkers

It is quite tricky to sense lung cancer biomarkers at the ppb level in real conditions, considering that they are blended with many other VOC including water at high concentration (more than 80 %). Still, detection of pure molecules must first be conducted before addressing a discriminating detection. Thus we have restricted the present study to the analysis of chemo-resistive properties of an array of RGO-CD based QRS in the presence of synthetic biomarkers produced under controlled conditions in the laboratory, being aware of the remaining possible obstacles until the final validation with cancerous patients. Among the several hundreds of cancer biomarkers produced by the body, we have selected the following ones, which are present in the breath of patients with lung cancer: acetone,[74] benzene,[74–76] methanol,[76]ethanol,[76] formaldehyde,[74] toluene,[74–76] xylene,[75] propanol,[74,77] isopropanol.[76] Relatively high contents of acetone (several ppm) are found because of a higher rate of oxidation of fatty acid under the conditions of oxidative stress. Aromatic hydrocarbons like benzene, toluene are also prominent lung cancer biomarker. Alcohols are abundant in the breath extract of both healthy subjects and lung cancer patients, but 1-propanol is found in the breath extract of lung cancer patients at higher concentration than healthy subjects.[74] This is the reason why an efficient detection and discrimination of alcohols, ketone bodies like acetone and aliphatic or aromatic hydrocarbons is required. Since breath extracts contain a huge amount of water tending to mask the trace amounts of VOC,[78] this molecule had also to be included into the selected set of VOC.

2.2. Synthesis and Fabrication of Sensors

The consideration of the wide range of polar/non-polar interactions possible with the selected biomarkers is justifying the varieties of transducers used (Table. 1):

✓ Reduced graphene oxide (RGO) will exhibit non-polar interactions and low disconnection capability, it is used as a reference,

✓ Pyrene adamantan linked RGO (RGO@PYAD) will increase junctions' gap due to PYAD spacer but is not expected to change selectivity,

✓ Native cyclodextrin linked RGO (RGO@PYAD-CD) is providing OH polar groups susceptible of interaction with polar analytes,

✓ Mannose functionalized cyclodextrin linked RGO (RGO@PYAD–MCD) providing OH polar groups with a longer spacer capable of easier disconnection,

✓ Amino functionalized cyclodextrin linked RGO (RGO@PYAD-NCD) is bringing reversible covalent bonding of its free amino group with acetone for instance,

✓ Perbenzylated cyclodextrin linked RGO (RGO@PBCD) is providing a strong non-polar character to the junction due to its numerous aromatic rings.

The variety of CD functionalization is a strong advantage, which makes this molecule an important brick in the sensors' design, allowing tailoring the junction's physico-chemical properties, i.e., the gap and the intermolecular interactions. Moreover, the association of functionalized CD with RGO foils is expected to preserve the accessibility of analytes to functional sites by maintaining a distance between foils that can be varied as a function of substituents' size and conformation. Additionally, an efficient connection between CD and RGO can be obtained with PYAD, resulting on one end from the fitting of the globular shape of adamantan (about 0.7 nm in diameter) inside the CD cage,[79] and on the other end from the π-π stacking of pyrene with graphene's surface.[80] Graphene oxide (GO) was synthesized from natural graphite powder by a modified HUMMER's method.[81] Thereafter, GO was non-covalently modified with PYAD, and then reduced to give RGO@PYAD, so that pyrene gets adsorbed on to the surface of graphene by π-π interaction. In the final step of synthesis, the functionalized cyclodextrin was allowed to interact with RGO@PYAD to induce a host-guest connection between the adamantan group and the cavity of cyclodextrin as shown in route a) of Fig. 1. For perbenzylated CD modified graphene, the step of adsorption of the linker was skipped, taking advantage of the π-π interaction between graphene and the aromatic residue of the CD according to route b) of Fig. 1. The characterizations of successful synthesis of functional cyclodextrins, and non-covalent modifications of graphene with functionalized cyclodextrins are available in the supporting information part (see Fig.S5 to Fig. S20).

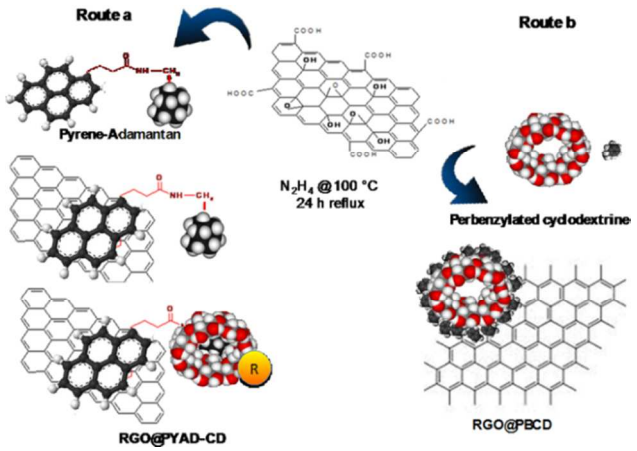

Fig. 1 Different routes of synthesis of functionalized cyclodextrin linked to reduced graphene oxide by supramolecular assembly. a) Route for the synthesis of RGO@PYAD-CD RGO@PYAD-MCD & RGO@PYAD-NCD (R is a hydroxyl group for CD, an amino group for NCD, and a mannose sugar for MCD), b) Route for the synthesis of RGO@PBCD.

View Article Online
DOI: 10.1039/C4TB01041H

The fabrication of QRS is a key point to ensure a good reproducibility of sensing performances. Firstly, the RGO decorated with different kinds of functionalized cyclodextrins needs to be efficiently dispersed in acetone with the aid of ultra-sonication for 1 h at 50 °C with a BRANSON 3510 device (100 W, 40 kHz), and secondly this well dispersed solution can be sprayed layer-by-layer (sLbL) onto inter-digitated electrodes.[82] Both the solutions' content and the number of sprayed layers allow to adjust the initial resistance of all the sensors to comparable values, so that only the chemical functionality of CD and not the transducer's percolation level,[83] will have an influence on sensors sensitivity to VOC. After fabrication, all sensors were conditioned in controlled atmosphere for one night before chemo-resistive tests.

Table 1 List of the fabricated sensors and their main characteristics

Sensor number	Description of the sensor	Designation of sensor	Structure of CD attached	Number of layers sprayed	Initial resistance of the sensor (R_0) kΩ
1	Reduced graphene oxide	RGO	N.A	8	120±4
2	Pyrene adamantan linked RGO	RGO@PYAD	N.A	9	130±6
3	Native cyclodextrin linked RGO	RGO@PYAD-CD	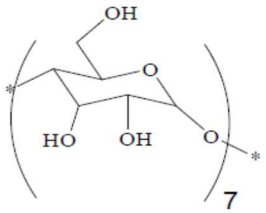	10	150±7
4	Mannose functionalized cyclodextrin linked RGO	RGO@PYAD–MCD	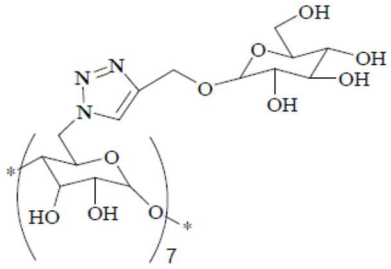	12	150±3
5	Amino functionalized cyclodextrin linked RGO	RGO@PYAD-NCD	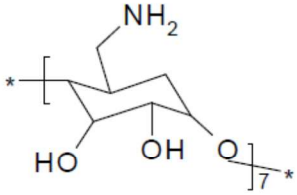	15	155±4
6	Perbenzylated cyclodextrin linked RGO	RGO@PBCD	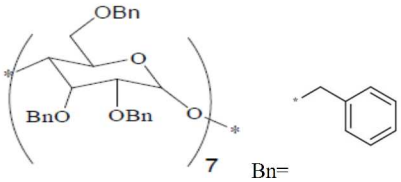 Bn=	10	125±5

2.3. Morphological Characterization

The technique consisting in the superimposition of layers of several tens of nm up to a final film thickness of some µm showed in Fig. 2a, has proved to allow the building of hierarchically structured transducers, which presents the advantage of bridging the original nanostructures developed by self assembly of RGO with CD, to the macroscopic parameter to measure (resistance variation). Atomic force microscopy (AFM) can give a good idea of the nano-structure obtained after sLbL in ambient conditions, using light tapping mode (TM-AFM) on a calibre multimode scanning probe microscope from BRUKER-VEECO, France. By comparing the images of Fig. 2b and Fig. 2c, one can notice a three times increase of graphene sheets' thickness in RGO@PBCD (around 3 nm) compared to GO (around 1.2 nm), which is comforting the idea that the decoration

View Article Online
DOI: 10.1039/C4TB01041H

of RGO with functionalized CD has been effective and useful to prevent the restacking of graphene sheets.

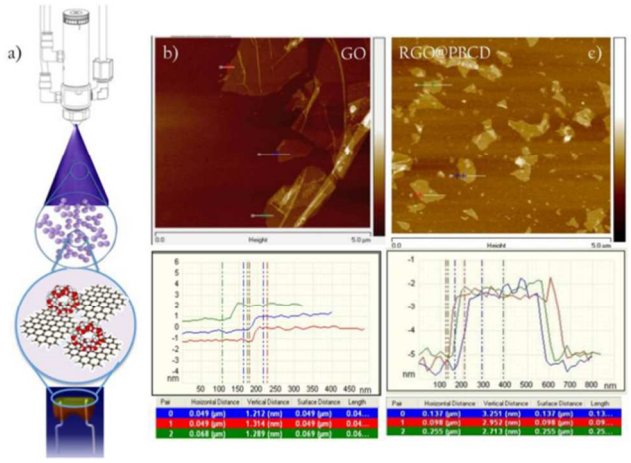

Fig. 2 (a) Scheme showing spray LbL deposition and AFM images of (b) GO and (c) RGO@PBCD

2.4. Sensing Performance of QRS

The chemo-resistive properties of the different CD functionalized RGO@PYAD sensors were then investigated by submitting them to a standard protocol developed in our group, which consists in successive expositions to rectangular pulses of 5 min in saturated VOC followed by 5 min in pure nitrogen. The control of the electrical valves adjusting the gas flows and data acquisition are both driven by a program developed under LabView environment as described in a previous publication.[84] The chemo-resistive responses of conductive CD nanocomposite (CCDC) sensors can be easily expressed by calculating the relative amplitude of electrical signals (A_r) towards solvents using Equation 1:

$$\boldsymbol{Ar} = \frac{\boldsymbol{R-R_0}}{\boldsymbol{R_0}} \quad \text{..... (1)}$$

where R_0 and R are the initial resistance of the sensor in pure nitrogen and the resistance of the sensor in the presence of solvent vapour, respectively.

The same volume of each vapour under saturated condition does not contain the same number of molecules due to differences in saturation vapour pressure of each analyte. Hence, in order to get rid of the influence of the number of molecules, response amplitude was normalized by a factor related to number of analyte molecules, following Equation 2, when partially selective response of each sensor to different VOC was compared.

$$Ar_{normalized} = \frac{\mathrm{Ar}}{[\mathrm{Analyte}]_{\mathrm{sat}}^{\mathrm{T,p}}} * 10^5 \quad \text{..... (2)}$$

Where $[\mathrm{Analyte}]_{sat}$ is the concentration of analyte molecules at saturation, T = 25 °C and p = 0.098 MPa

For experiments in the ppm-ppb range another device was used to control VOC concentrations by combining LabView and OVG-4 softwares. This accurate chemical vapour generator is composed of an oven and a controller of both sample and split flows. The sample flow was kept at 100 $cm^3.min^{-1}$ whereas the split flow was varied to change the VOC concentration at a fixed temperature of 25 °C.

2.4.1. Chemo-electrical behaviour

The bar graph of Fig. 3a gives a good overview of the e-nose's fingerprint (assembled with RGO, RGO@PYAD, RGO@PYAD-CD, RGO@PYAD-MCD, RGO@PYAD-NCD, RGO@PBCD sensors, see Table. 1 for details about the sensors composition), when exposed to a set of 10 VOC (methanol, ethanol, propanol, isopropanol, benzene, toluene, p-xylene, acetone, formaldehyde which have been selected among lung cancer biomarkers, plus water which is present in breath at more than 90 %, (see Table S2 in supplementary information for details about solubility parameters of these solvents). Looking at Fig. 3a in more details shows the selectivity of the different sensors and also allows noticing their non-specificity (they all respond to all VOC but not with the same segregation ability, as it is the case for the olfactory receptors of mammal nostrils). As shown in supplementary information (Fig. S21) the resistance variation of CCDC sensors is sharp upon exposure to VOC (some seconds only are necessary to reach signals' saturation), stable and reversible (recovery of the initial value of the resistance R_0, before the end of the dry nitrogen purge cycle).

As postulated before, the sensitivity/selectivity of each sensor can be interpreted as a function of the modification of junctions' physico-chemical properties. In this study two main parameters can significantly affect junctions to promote tunneling to the detriment of ohmic conduction in the CCDC network, the steric hindrance of linkers and their ability to adsorb analytes that will expand the junctions. This last parameter is in turn related to the functionality of the CD. For instance the slightly higher sensitivity of RGO@PYAD than RGO must be due to a better exfoliation of the graphene sheets due to PYAD spacing that is preventing at the same time the restacking of foils. However it can be noticed that PYAD is not changing the selectivity of pristine graphene, meaning that this molecule is not specifically interacting with any of the studied VOC. The best selectivity of RGO@PYAD-CD towards polar VOC (although of low magnitude) can be explained by the presence of several hydroxyl groups on native CD. Moreover the fact that RGO@PYAD-MCD, RGO@PYAD-NCD and RGO@PBCD have different selectivity than RGO@PYAD-CD is a confirmation of the effectiveness of the strategy chosen in this work to tailor the sensors' selectivity, i.e., changing its van der Waals interactions with the analytes by CD functionalization. Nevertheless, the strong sensitivity of RGO@PYAD-NCD sensors to acetone vapour is more likely coming from its free amino group in RGO@PYAD-NCD that might have undergone a reversible imine formation reaction with acetone, and not from specific van der Waals interactions. The ranking of sensitivity to VOC of RGO@PBCD deduced from Fig. 3a is: benzene> toluene > p-xylene> isopropanol> propanol> ethanol> acetone> methanol> water> formaldehyde is consistent with the fact the perbenzylation of β-CD enhances the affinity of RGO@PBCD for non-polar VOC. Reversely the ranking of sensitivity to VOC of RGO@PYAD-MCD sensors is demonstrating a higher affinity for polar vapours, i.e., methanol > ethanol > propanol > isopropanol > water > benzene > toluene > p-xylene > acetone > formaldehyde. In this case the presence of triazole rings and free hydroxide groups (of the sugar residue) in the MCD can explain

Dynamic Article Links ►
View Article Online
DOI: 10.1039/C4TB01041H

Cite this: DOI: 10.1039/c0xx00000x

www.rsc.org/xxxxxx

ARTICLE TYPE

the enhancement of affinity of this sensor for polar solvents, especially alcohols, thanks to the possibility of hydrogen bonding. Furthermore, it can be noticed distinctly that RGO@PYAD-MCD sensors are able to discriminate alcohols, depending on their number of carbon atoms. Hence, in this case the analytes' size might also contribute to the selectivity of sensors.

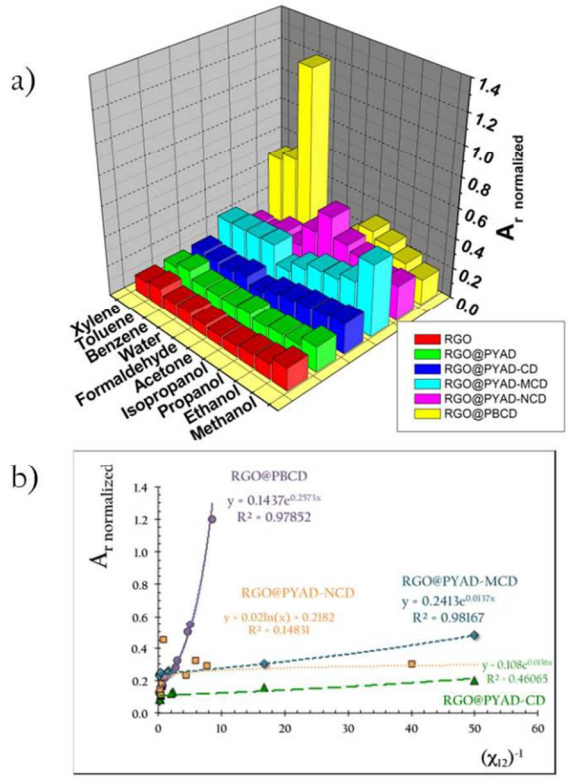

Fig. 3. a) Normalized average maximum relative amplitude of an array of 6 sensors towards 10 VOC and b) correlation between χ_{12} parameter and transducer's selectivity for RGO@PBCD, RGO@PYAD-NCD, RGO@PYAD-MCD and RGO@PYAD-CD

2.4.2. Origin of selectivity

As intuited in an early work [85] and confirmed later, [35,43] the van der WAALS interaction between the chemical groups present in the CCDC and in the VOC can be correlated to the amplitude of their chemo-resistive response Ar, thus explaining the selectivity of CCDC sensors provided that no stronger effect interferes, such as size of analytes or stronger interactions (ionic, or covalent bonding). When these constraints are satisfied, secondary interactions between molecules can be well described by the FLORY-HUGGINS interaction parameter (χ_{12}). χ_{12} is expected to tend to zero in case of strong secondary interactions that correspond also to high values of A_r. Normally for CPC vapour QRS, A_r increases exponentially with the inverse of χ_{12} according to Equation 3, but is it the same in CCDC in which the polymer phase is replaced by functionalized CD?

$$Ar_{normalized} = a.e^{\frac{b}{\chi_{12}}} \quad \text{.....(3)}$$

With χ_{12} the Flory-Huggins intermolecular interaction parameter which can be determined using Equation 4, a and b are constants

$$\boldsymbol{\chi_{12} = V_m RT(\delta_{Tpol} - \delta_{Tsol})^2} \quad \text{..... (4)}$$

where V_m is molar volume of solvent, T is temperature in Kelvin, R is universal gas constant and $\delta_{T\ pol}$ and $\delta_{T\ sol}$ are polymer and solvent total solubility parameter respectively

To check that functionalized cyclodextrins, which can be considered as oligomers, satisfy also the FLORY-HUGGINS approach, the global solubility parameter δ_T of four of them, i.e., CD, MCD, PBCD and NCD, have been evaluated by the FEDORS' method of groups' contribution.[86] The following values of δ_T were found respectively 27.6, 28.3, 20.29 and 25.9 J ^{½}.cm$^{-3/2}$, allowing to calculate the corresponding χ_{12} parameters using Equation 4 (detailed values are given in Table S2 of supporting information). The validity of the model can then be evaluated by plotting the evolution of the normalized relative amplitude Ar of RGO@PBCD, RGO@PYAD-NCD, RGO@PYAD-MCD and RGO@PYAD-CD transducers with $1/\chi_{12}$ using Equation 3**.** The resulting curves plotted in Fig. 3b, show that three over the four sensors, i.e., RGO@PBCD, RGO@PYAD-MCD and RGO@PYAD-CD are well fitting the exponential law, whereas RGO@PYAD-NCD evolution seems to be better described by a logarithm. Comparing the curves of RGO@PYAD-CD and RGO@PYAD-MCD shows that they can almost be superimposed by translation, which means that they have quite the same discrimination ability due to similar interactions with analytes, RGO@PYAD-MCD being always more sensitive probably because of the larger size of its spacer, making more easy the disconnection of junctions. The larger slope of RGO@PBCD compared to that of RGO@PYAD-MCD demonstrates the superior discrimination ability of the former, which appears to offer a better compromise between selectivity and sensitivity. The peculiar behaviour of RGO@PYAD-NCD, which is not following the same law as the other sensors, seems to confirm the possibility of a chemo-resistive response based on molecular recognition by the reversible reaction of the amine function of NCD that can form an imine with analytes such as acetone. Thus, this chemo-resistive behaviour must not be mainly based on weaker van der WAALS interactions. Therefore it can be concluded that the decoration of graphene platelets with different types of cyclodextrins is an effective strategy to tailor the sensors' selectivity to VOC, simply by changing the chemical nature of the functions present on CD.

2.4.3. Performance of the sensor array in an electronic nose

To illustrate the discrimination ability of functionalized cyclodextrin decorated graphene sensors, an array of three CCDC

View Article Online
DOI: 10.1039/C4TB01041H

sensors, namely RGO@PYAD-MCD, RGO@PYAD-NCD and RGO@PBCD, was assembled in an e-nose and exposed to the same set of 10 VOC biomarkers as previously. For each analyte, five VOC/nitrogen successive sequences were recorded and all signals' maxima were collected into an m by n matrix (m being the number of measurements and n the number of sensors), and subsequently treated with a principal component analysis (PCA) algorithm implemented in the TANAGRA software [87] PCA is a simple and effective method that makes a multi-dimensional mapping of data onto 3 axes with a minimum loss of information. As shown by the pattern of Fig. 4a, the two first principal components (PC1, PC2) obtained scores of 60.75 and 25.55 respectively, accounting for 86.28 % of the total variance. This is a quite good result considering that only three sensors were used in this e-nose compared to several tens in some devices. Additionally, the clusters of points corresponding to target analytes are clearly well separated, which confirms that the CCDC sensors are effective to distinguish the ten VOC biomarkers. The PCA map is also showing the ability of the e-nose to discriminate specific lung cancer biomarker as 2-propanol from other alcoholic VOC and even water, which are abundant in breath extract.

2.4.4. Limit of detection

The organic vapour flow rate was varied by blending mixtures of saturated VOC and dry nitrogen at different ratios. In this way the analyte flow rate was varied from 20 to 100 $cm^3.min^{-1}$, which corresponds to variation or the solvent fraction from 0.2 to 1 (the concentration of benzene at saturated is 147088 ppm), keeping the total flow rate constant at 100 $cm^3.min^{-1}$. It can be clearly seen in Fig. 4b that the amplitude of the chemo-resistive responses Ar of the set of CCDC sensors is regularly increasing with the amount of benzene molecules in their surrounding. None of the curves are found to cross each others, which attests that their ranking of selectivity is kept in the whole range of analyte concentration. Thus all sensors can be considered as operational over a wide range of concentration of VOC from the some hundred of ppb to slightly more than a thousand hundred ppm.

Moreover, since all the lung cancer VOC biomarker found in breath extract are usually present at some ppm (part per million) or even some ppb (part per billion), it is important to check that the limit of detection of CCDC sensors is compatible with such low concentrations. In order to assess the efficiency of the transducers to sense traces of analyte molecules in their surrounding, their signal to noise ratio (*SNR*) was calculated with Equation 5[88]

$$SNR = \frac{\Delta R_{max}}{\sigma_{baseline}} \text{..... (5)}$$

Where, ΔR_{max} or $A_{r\,max}$ is the steady-state resistance change of the sensor upon exposure to solvent vapour molecules (analyte), i.e., ratio between the maximum resistance and the baseline. $\sigma_{baseline}$ corresponds to the standard deviation in baseline resistance before analyte delivery, calculated using 10 data points as shown in supplementary information (Fig. S22).

The sensors' signals can be considered as valid if, for a defined concentration of VOC (analyte), their SNR is higher or equal to 2.0 (SNR ≥ 2.0). The calculation of S/N ratios for the RGO and RGO@PBCD responses shown in Fig. 4c corresponding to pulses of 400 ppb of benzene vapour was found to give 11 and 88 respectively. This demonstrates that, the noise density of RGO sensor has reduced significantly after being wrapped by perbenzyle cyclodextrin (PBCD) along with enhancement of sensitivity of the sensor.

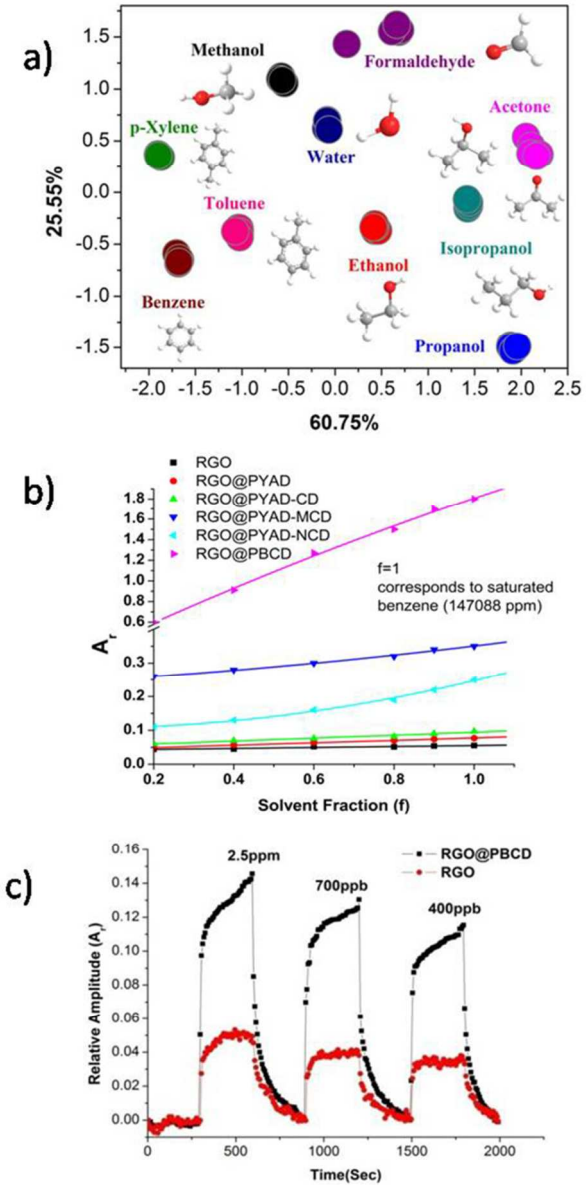

Fig.4. a) Pattern recognition of the electronic nose exposed to a set of lung cancer biomarker VOC after principal component analysis (PCA), b) Chemo-resistive responses of a set of CCDC sensors to benzene vapour for varying analyte flow rates (lines have been drawn to guide the eyes), c) Responses of RGO@PBCD and RGO sensors to benzene vapour in the ppm-ppb concentration range

III. Conclusion

Our study is opening a novel approach to control the multiscale architecture of quantum chemo-resistive transducers by the supramolecular assembly of graphene and CD-derivate

Dynamic Article Links ►
View Article Online
DOI: 10.1039/C4TB01041H

Cite this: DOI: 10.1039/c0xx00000x

www.rsc.org/xxxxxx

ARTICLE TYPE

hybrids. This strategy allows to get a high sensitivity of the nanoswitching at junctions due to the insertion of CD between graphene foils and to obtain a tailorable selectivity to cancer biomarkers due to CD functionalization and geometry. The resulting CCDC QRS have demonstrated a high sensitivity, evidenced by SNR up to 88 at a concentration as low as 400 ppb without any preconcentration of vapours or amplification of signals. These sensors also proved to have good discrimination ability towards the ten lung cancer VOC biomarkers studied, which could interestingly be predicted by a model based on van der WAALS interactions, excepted in case of a covalent bonding used for molecules' recognition (acetone). These findings are promising to switch to the next step, i.e., the confrontation of e-noses to real VOC biomarkers present in patients' breath in order to make an anticipated diagnosis of cancers.

Notes and references

[a] Smart Plastics Group, European University of Brittany (UEB), LIMAT[B]-UBS, Lorient 56321, France; E-mail: jean-francois.feller@univ-ubs.fr

[b] *Centre for Polymer Science & Engineering, Indian Institute of Technology, Delhi-110016, India*

[c] *Lab. of Analysis & Modelling for Biology & Environment (LAMBE-UMR 8587), University of Evry, 91025 Evry Cedex, France;*

[d] Sorbonne Universités, UPMC Univ. Paris 06, 75005 Paris Cedex, France ; E-mail: philippe.guegan@upmc.fr

[e] *CNRS, UMR 8232, IPCM, Chimie des Polymères, 75005 Paris, France*

† Electronic Supplementary Information (ESI) available: [details of synthesis and characterizations of functionalized cyclodextrins and reduced graphene oxide wrapped functionalized cyclodextrins are available in supplementary information]. See DOI: 10.1039/b000000x/

1. *Cent. Dis. Control Prev.*, 2014.
2. B. de Lacy Costello, A. Amann, H. Al-Kateb, C. Flynn, W. Filipiak, T. Khalid, D. Osborne, and N. M. Ratcliffe, *J. Breath Res.*, 2014, **8**, 014001.
3. Y. Y. Broza, L. Zuri, and H. Haick, *Sci. Rep.*, 2014, **4**, 1–6.
4. A. Manolls, *Clin. Chem.*, 1983, **29**, 5–15.
5. M. Phillips, K. Gleeson, J. M. Hughes, J. Greenberg, R. N. Cataneo, L. Baker, and W. P. McVay, *Lancet*, 1999, **353**, 1930–1933.
6. J. W. Gardner, H. W. Shin, and E. L. Hines, *Sensors Actuators B Chem.*, 2000, **70**, 19–24.
7. G. Peng, U. Tisch, O. Adams, M. Hakim, N. Shehada, Y. Y. Broza, S. Billan, R. Abdah-Bortnyak, A. Kuten, and H. Haick, *Nat Nano*, 2009, **4**, 669–673.
8. N. G. Hockstein, E. R. Thaler, D. Torigian, W. T. Miller, O. Deffenderfer, and C. W. Hanson, *Laryngoscope*, 2004, **114**, 1701–1705.
9. R. Ionescu, Y. Broza, H. Shaltieli, D. Sadeh, Y. Zilberman, X. Feng, L. Glass-Marmor, I. Lejbkowicz, K. Müllen, A. Miller, and H. Haick, *ACS Chem. Neurosci.*, 2011, **2**, 687–93.
10. M. McCulloch, T. Jezierski, M. Broffman, A. Hubbard, K. Turner, and T. Janecki, *Integr. Cancer Ther.*, 2006, **5**, 30–9.
11. G. Peng, M. Hakim, Y. Y. Broza, S. Billan, R. Abdah-Bortnyak, A. Kuten, U. Tisch, and H. Haick, *Br. J. Cancer*, 2010, **103**, 542–551.
12. C. L. Silva, M. Passos, and J. S. Câmara, *Talanta*, 2012, **89**, 360–8.
13. A. P. F. Turner and N. Magan, *Nat Rev Micro*, 2004, **2**, 161–166.
14. H. J. O'Neill, S. N. Gordon, M. H. O'Neill, R. D. GIbbons, and J. P. Szldon, *Clin. Chem.*, 1988, **34**, 1613–1618.
15. G. Giubileo, *Proc. SPIE*, 2002, **4762**, 318–325.
16. D. Smith, T. Wang, J. Sulé-Suso, P. Spanel, and A. El Haj, *Rapid Commun. Mass Spectrom.*, 2003, **17**, 845–50.
17. M. J. Thorpe, D. Balslev-Clausen, M. S. Kirchner, and J. Ye, *Opt. Express*, 2007, **16**, 6–15.
18. A. D'Amico, G. Pennazza, M. Santonico, E. Martinelli, C. Roscioni, G. Galluccio, R. Paolesse, and C. Di Natale, *Lung cancer*, 2010, **68**, 170–6.
19. H.T.Nagle, R.G.Osuna, and S.S.Schiffman, *IEEE Spectr.*, 1998, **35**, 22–31.
20. S. Dragonieri, M. P. van der Schee, T. Massaro, N. Schiavulli, P. Brinkman, A. Pinca, P. Carratú, A. Spanevello, O. Resta, M. Musti, and P. J. Sterk, *Lung Cancer*, 2012, **75**, 326–31.
21. M. M. Arafat, B. Dinan, S. A. Akbar, and A. S. M. A. Haseeb, *Sensors*, 2012, **12**, 7207–58.
22. C. Wang, L. Yin, L. Zhang, D. Xiang, and R. Gao, *Sensors*, 2010, **10**, 2088–106.
23. J. Lu, B. J. Park, B. Kumar, M. Castro, H. J. Choi, and J. F. Feller, *Nanotechnology*, 2010, **21**, 1–10.
24. Y. Dan, Y. Cao, T. E. Mallouk, S. Evoy, and A. T. C. Johnson, *Nanotechnology*, 2009, **20**, 434014.
25. B. Kumar, M. Castro, and J. F. Feller, *Sensors Actuators B Chem.*, 2012, **161**, 621–628.
26. J. Lu, J. F. Feller, B. Kumar, M. Castro, Y. S. Kim, Y. T. Park, and J. C. Grunlan, *Sensors Actuators B Chem.*, 2011, **155**, 28–36.
27. A. Bouvree, J. F. Feller, M. Castro, Y. Grohens, and M. Rinaudo, *Sensors Actuators B Chem.*, 2009, **138**, 138–147.
28. G. Peng, E. Trock, and H. Haick, *Nano Lett.*, 2008, **8**, 3631–3635.
29. G. Peng, U. Tisch, and H. Haick, *Nano Lett.*, 2009, **9**, 1362–1368.
30. C. Wang, L. Yin, L. Zhang, D. Xiang, and R. Gao, *Sensors*, 2010, **10**, 2088–2106.
31. H. Bai and G. Shi, *Sensors*, 2007, **7**, 267–307.
32. J. Lu, B. Kumar, M. Castro, and J. F. Feller, *Sensors Actuators B Chem.*, 2009, **140**, 451–460.
33. J. F. Feller, J. Lu, K. Zhang, B. Kumar, M. Castro, N. Gatt, and H. J. Choi, *J. Mater. Chem.*, 2011, **21**, 4142.
34. B. Kumar, M. Castro, and J. F. Feller, *Carbon N. Y.*, 2012, **50**, 3627–3634.
35. B. Kumar, M. Castro, and J. F. Feller, *J. Mater. Chem.*, 2012, **22**, 10656.
36. B. Kumar, M. Castro, and J. F. Feller, *Chem. sensors*, 2013, **3**, 41–44.
37. S. Chatterjee, M. Castro, and J. F. Feller, *J. Mater. Chem. B*, 2013, **1**, 4563.
38. T. T. Tung, M. Castro, T. Y. Kim, K. S. Suh, and J. F. Feller, *J. Mater. Chem.*, 2012, **22**, 21754–21766.
39. B. Kumar, M. Castro, and J. F. Feller, *J. Mater. Chem.*, 2012, **22**, 10656–10664.
40. B. Kumar, M. Castro, and J. F. Feller, *Carbon N. Y.*, 2012, **50**, 3627–3634.
41. J. F. Feller, N. Gatt, B. Kumar, and M. Castro, *ChemoSensors*, 2014, **2**, 26–40.
42. M. Castro, J. Lu, S. Bruzaud, B. Kumar, and J. F. Feller, *Carbon N. Y.*, 2009, **47**, 1930–1942.
43. B. Kumar, J. F. Feller, M. Castro, and J. Lu, *Talanta*, 2010, **81**, 908–15.
44. A. Bouvrée, J. F. Feller, M. Castro, Y. Grohens, and M. Rinaudo, *Sensors Actuators B Chem.*, 2009, **138**, 138–147.
45. B. Kumar, M. Castro, and J. F. Feller, *Carbon N. Y.*, 2012, **50**, 3627–3634.

View Article Online
DOI: 10.1039/C4TB01041H

46. R. Ionescu, Y. Broza, H. Shaltieli, D. Sadeh, Y. Zilberman, X. Feng, L. Glass-Marmor, I. Lejbkowicz, K. Müllen, A. Miller, and H. Haick, *ACS Chem. Neurosci.*, 2011, **2**, 687–693.
47. N. Bachar, L. Mintz, Y. Zilberman, R. Ionescu, X. Feng, K. Müllen, and H. Haick, *ACS Appl. Mater. Interfaces*, 2012, **4**, 4960–4965.
48. E. Massera, a. Castaldo, L. Quercia, and G. Di Francia, *Sensors Actuators B Chem.*, 2008, **129**, 487–490.
49. Y. Zilberman, U. Tisch, G. Shuster, W. Pisula, X. Feng, K. Müllen, and H. Haick, *Adv. Mater.*, 2010, **22**, 4317–4320.
50. N. G. Sahoo, S. Rana, J. W. Cho, L. Li, and S. H. Chan, *Prog. Polym. Sci.*, 2010, **35**, 837–867.
51. K. S. Novoselov, *Science.*, 2004, **306**, 666–669.
52. R. F. Service, *Science.*, 2009, **324**, 875–877.
53. A. A. Balandin, S. Ghosh, W. Bao, I. Calizo, D. Teweldebrhan, F. Miao, and C. N. Lau, *Nano Lett.*, 2008, **8**, 902–7.
54. C. Lee, X. Wei, J. W. Kysar, and J. Hone, *Science.*, 2008, **321**, 385–8.
55. J. Hass, W. A. de Heer, and E. H. Conrad, *J. Phys. Condens. Matter*, 2008, **20**, 323202.
56. J. D. Fowler, M. J. Allen, V. C. Tung, Y. Yang, R. B. Kaner, B. H. Weiller, Ḱ. M. J. Allen, and Ḱ. V. C. Tung, *ACS Nano*, 2009, **3**, 301–306.
57. F. Schedin, A. K. Geim, S. V Morozov, E. W. Hill, P. Blake, M. I. Katsnelson, and K. S. Novoselov, *Nat Mater*, 2007, **6**, 652–655.
58. K. S. Novoselov, A. K. Geim, S. V Morozov, D. Jiang, M. I. Katsnelson, I. V Grigorieva, S. V Dubonos, and A. A. Firsov, *Nature*, 2005, **438**, 197–200.
59. A. K. Geim and K. S. Novoselov, *Nat Mater*, 2007, **6**, 183–191.
60. B. Zhang, Q. Li, and T. Cui, *Biosens. Bioelectron.*, 2012, **31**, 105–9.
61. T. T. Tung, M. Castro, T. Y. Kim, K. S. Suh, and J. F. Feller, *J. Mater. Chem.*, 2012, **22**, 21754.
62. P. Shahgaldian and U. Pieles, *Sensors*, 2006, **6**, 593–615.
63. M. V. Rekharsky and Y. Inoue, *Chem. Rev.*, 1998, **98**, 1875–1918.
64. V. Monnaert, D. Betbeder, L. Fenart, H. Bricout, A. M. Lenfant, C. Landry, R. Cecchelli, E. Monflier, and S. Tilloy, *J. Pharmacol. Exp. Ther.*, 2004, **311**, 1115–1120.
65. N. Badi, P. Guégan, F.-X. Legrand, L. Leclercq, S. Tilloy, and E. Monflier, *J. Mol. Catal. A Chem.*, 2010, **318**, 8–14.
66. I. Tabushi, Y. Kuroda, and K. Yokota, *Tetrahedron Lett.*, 1982, **23**, 4601–4604.
67. T. Ogoshi and A. Harada, *Sensors*, 2008, **8**, 4961–4982.
68. Y. Guo, S. Guo, J. Ren, Y. Zhai, S. Dong, and E. Wang, *ACS Nano*, 2010, **4**, 4001–4010.
69. B. Léger, S. Menuel, D. Landy, J. F. Blach, E. Monflier, and A. Ponchel, *Chem. Commun.*, 2010, **46**, 7382–4.
70. L. Kong, J. Wang, F. Meng, X. Chen, Z. Jin, M. Li, J. Liu, and X.-J. Huang, *J. Mater. Chem.*, 2011, **21**, 11109.
71. L. Li, W. Feng, and P. Ji, *Bioeng. Food, Nat. Prod. Protein*, 2011, **57**, 3507–3513.
72. L. Yang, Y. Xu, X. Wang, J. Zhu, R. Zhang, P. He, and Y. Fang, *Anal. Chim. Acta*, 2011, **689**, 39–46.
73. Z. Guo, Y. Feng, D. Zhu, S. He, H. Liu, X. Shi, J. Sun, and M. Qu, *Adv. Funct. Mater.*, 2013, **23**, 5010–5018.
74. M. Hakim, Y. Y. Broza, O. Barash, N. Peled, M. Phillips, A. Amann, and H. Haick, *Chem. Rev.*, 2012, **112**, 5949–5966.
75. D. Poli, P. Carbognani, M. Corradi, M. Goldoni, O. Acampa, B. Balbi, L. Bianchi, M. Rusca, and A. Mutti, *Respir. Res.*, 2005, **6**, 71.
76. R. F. Machado, D. Laskowski, O. Deffenderfer, T. Burch, S. Zheng, P. J. Mazzone, T. Mekhail, C. Jennings, J. K. Stoller, J. Pyle, J. Duncan, R. A. Dweik, and S. C. Erzurum, *Am. J. Respir. Crit. Care Med.*, 2005, **171**, 1286–91.
77. S. M. Gordon, J. P. Szldon, B. K. Krotoszynski, R. D. Gibbons, and J. O. Neill, *Clin. Chem*, 1985, **1282**, 1278–1282.
78. S. M. Cho, Y. J. Kim, G. S. Heo, and S.-M. Shin, *Sensors Actuators B Chem.*, 2006, **117**, 50–57.
79. R. Haddad, M. Holzinger, R. Villalonga, A. Neumann, J. Roots, a. Maaref, and S. Cosnier, *Carbon N. Y.*, 2011, **49**, 2571–2578.
80. Y.-L. Zhao, L. Hu, J. F. Stoddart, and G. Grüner, *Adv. Mater.*, 2008, **20**, 1910–1915.
81. William S. Hummers and R. E. Offeman, *J. Am. Chem. Soc.*, 1958, **80**, 1339–1339.
82. J. F. Feller, B. Kumar, and M. Castro, in *Nanocomposites with biodegradable polymers: Synthesis, Properties & Future Perspectives*, ed. V. Mital, Oxford University Press, Oxford (UK), 1st edn., 2011, pp. 368–399.
83. J. Lu, B. Kumar, M. Castro, and J. F. Feller, *Sensors Actuators B Chem.*, 2009, **140**, 451–460.
84. N. Bachar, L. Mintz, Y. Zilberman, R. Ionescu, X. Feng, K. Müllen, and H. Haick, *ACS Appl. Mater. Interfaces*, 2012, **4**, 4960–5.
85. J. F. Feller and Y. Grohens, *Sensors Actuators B Chem.*, 2004, **97**, 231–242.
86. Fedors, *Polym Eng Sci.*, 1974, **14**, 147–154.
87. R. Rakotomalala, *EGC'2005 Proc.*, 2005, **2**, 697–702.
88. T. Gao, M. D. Woodka, B. S. Brunschwig, and N. S. Lewis, *Chem. Mater.*, 2006, **18**, 5193–5202.